

NMR investigation of the electronic structure of the RbC_{60} polymer phase

K.-F. Thier, G. Zimmer, and M. Mehring

2. Physikalisches Institut, Universität Stuttgart, Pfaffenwaldring 57, D-70550 Stuttgart, Federal Republic of Germany

F. Rachdi

Groupe de Dynamique des Phases Condensées, Université des Sciences et Technique du Languedoc, 34060 Montpellier, France

(Received 16 October 1995)

We present ^{13}C high-resolution NMR data on the low-temperature (polymeric) phase of RbC_{60} . From the temperature-dependent line shift we have extracted information about the hyperfine couplings and electron density distribution on the C_{60} molecules. The data also support the existence of an sp^3 -like bonding type between the molecules.

Among the manifold of the different alkali-metal doped C_{60} materials A_xC_{60} ($\text{A}=\text{Cs}, \text{Rb}, \text{K}$) the recently discovered AC_{60} phases^{1–4} attracted special interest because of their complex and varying phase diagrams. Besides the high-temperature fcc phase a polymeric phase⁵ below 390 K exists, where the C_{60} molecules are thought to form one-dimensional chains. Below 50 K RbC_{60} is proposed to exhibit a phase transition into a magnetically ordered state.⁶ Recently also different metastable phases^{3,4,7} were discovered, one of them was attributed to the formation of dimers.^{6,8–10} Although the existence of the polymeric and the ordered low-temperature phases is now well established, many questions concerning their electronic structure, i.e., dimensionality and the kind of magnetic coupling of the electrons, are still under discussion. In this contribution we want to address this point using NMR as a local probe for determining the electronic structure of RbC_{60} .

The sample with a nominal RbC_{60} composition was prepared using standard procedures.¹¹ NMR spectroscopy showed a small Rb underdoping leading to excess $\alpha\text{-C}_{60}$. The air stability of the sample was tested by exposing the sample to air after a series of magic angle spinning (MAS) spectra had been taken: no changes in the MAS-NMR spectrum could be detected after several days of air contact.

All MAS experiments were performed on home built NMR spectrometers operating at ^{13}C Larmor precession frequencies of 83.7 and 45.6 MHz. The spectra were obtained by a Hahn echo sequence with the echo delay times adjusted to a rotor period. The spinning speed varied from 8 kHz at 300 K to 7 kHz at 100 K. Variable temperatures were achieved by using cold nitrogen gas for drive and bearing. Referenced temperatures refer to the temperature of the bearing gas before entering the stator. The spinning speed was controlled electronically and spin rate oscillations were less than 2 Hz.

The upper trace in Fig. 1(a) shows the ^{13}C MAS spectrum at room temperature. Besides the narrow line at 143 ppm which is due to excess $\alpha\text{-C}_{60}$, nine additional lines from RbC_{60} can be identified. We assign lines 1–8 to the polymeric phase. The narrow line at 179 ppm is identical with the shift of the fcc high-temperature phase. Also its spin lattice relaxation time of 70 ms coincides with the values found in the high-temperature phase. We therefore consider its inten-

sity (about 2 %) as a small remainder of the fcc phase. Interestingly enough, this is not due to quenching or hysteresis effects: the intensity of the fcc line completely vanishes when cooling the sample further down, but returns in a reversible way when warming up to room temperature again.

We note that the temperature-dependent measurements are important for the separation of lines 5–8. At a single temperature, an assignment of all lines is not possible because of the large overlap in the region around 50 ppm. The lines show substantial broadening, which limits the resolution severely. The broadening arises partly because most of

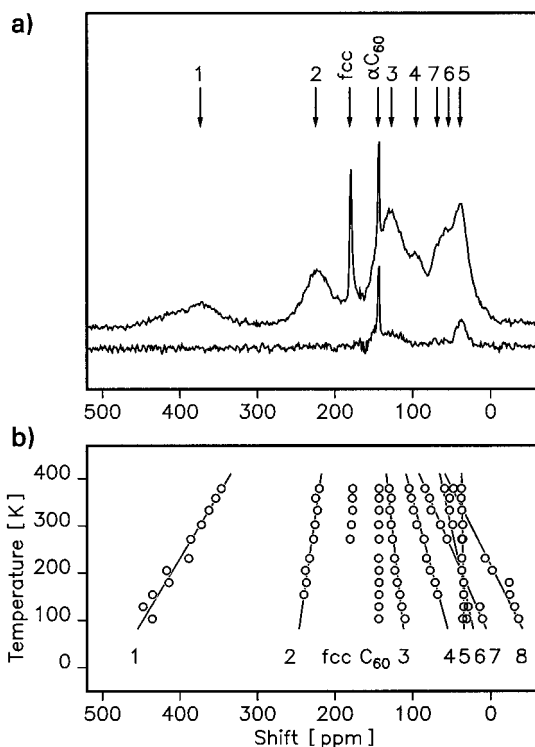


FIG. 1. (a) ^{13}C MAS-NMR spectrum at room temperature after 4 s recovery time. Bottom: spectrum of only the slow relaxing parts which was obtained by subtracting the spectrum after 1 s recovery time from the upper one after 4 s recovery time. (b) Temperature dependence of the lines in the region of 100–370 K.

TABLE I. Intensity, hyperfine coupling, and relaxation rates of lines 1–8.

Pos.	Int.	a_{iso} (MHz)	T_1^{-1} (s ⁻¹)
1	8	7.6	33
2	8	2.2	9
3	24	-1.4	2.7
4	2	-3.4	
5	4	-0.2	0.5
6	8	-2.7	4.2
7	2	-5.5	
8	4	-6.3	

the assigned lines consist of a distribution of lines belonging to different sites. Other broadening effects are probably due to disorder. The characteristic feature of the spectrum of the orthorhombic phase—in contrast to α -C₆₀ and to the high-temperature fcc phase—is the wide distribution of isotropic shifts. In order to understand the origin of this shift distribution, we have to separate the resonance shift δ into two contributions: the Knight shift K and the chemical shift σ :

$$\delta = \sigma + K. \quad (1)$$

While the chemical shift is due to the electronic structure of the closed shells and indicative of the chemical environment of a specific carbon site, the Knight shift is proportional to the hyperfine interaction a and spin polarization χ_s of the delocalized π electrons. The two shift contributions can be separated by their temperature dependence. Whereas the chemical shift is expected to depend only weakly on temperature, the Knight shift follows χ_s according to

$$\frac{dK}{dT} = (\hbar \gamma_n \gamma_e)^{-1} a \frac{d\chi_s}{dT}. \quad (2)$$

Using relation (2), we can extract directly the hyperfine coupling constants for the different peaks without knowing the chemical shift values.

Figure 1(b) shows the temperature dependence of the lines assigned to the orthorhombic phase. Note that with increasing temperature all lines seem to shift closer to the line of pure C₆₀ at 143 ppm. ESR measurements⁷ show a decrease in spin susceptibility in this temperature range. The ¹³C shift distribution therefore arises primarily from a broad distribution of Knight shifts and consequently the chemical shift tensor of the majority of the carbon sites is not strongly influenced by the crystal structure.¹² This is also consistent with NMR results in other A_xC₆₀ materials where the chemical shift changes only slightly by about 2 ppm per charge on the C₆₀ molecule.¹³ From the spin susceptibility data in Ref. 7 follows a temperature dependence of $d\chi_s/dT = 5.89 \times 10^{-7}$ emu/(mol K). Applying this value to our data we obtain the hyperfine coupling constants listed in Table I. Assuming that all carbons are visible in the MAS spectra, we also tried to fit the relative intensities of the different lines. With the additional assumption, that at least two carbon positions on the C₆₀ molecule have the same isotropic shifts, due to a symmetry plane, the best results obtained for the intensity ratios are also given in Table I.

According to the proposed polymeric structure of the orthorhombic phase⁵ one would expect sp^3 -like carbons at the connecting sites in the C₆₀ molecule. A characteristic property of sp^3 carbons in NMR spectroscopy is its small isotropic chemical shift and a small chemical shift anisotropy. Known isotropic chemical shift values for quaternary carbons are typically in the region 37 ± 5 ppm.¹⁴ We pointed out earlier^{11,15} that the MAS spectra of RbC₆₀ as well as KC₆₀ show spectral intensity in this region. From the analysis of the temperature dependence of the lines it follows, however, that most of the intensity in this region is due to negative Knight shifts and chemical shifts close to the values of α -C₆₀. An exception is line 5, which has only a very small hyperfine contribution and its chemical shift value can be estimated to be close to 40 ppm. Note that four sp^3 carbons per C₆₀ molecule should add up to about 6.7 % of the total intensity, a value that turns out to be in good agreement with the intensity of line 5.

At all temperatures, also spin lattice relaxation was measured using the saturation-recovery technique. Whereas the relaxation rates vary strongly for the different lines, no observable temperature dependence could be detected between 100 and 370 K. This agrees with the results of static powder measurements.¹⁶ The values in Table I were obtained using a monoexponential fit routine for lines 1–3. The magnetization-recovery curves of all lines, however, were not purely monoexponential and especially in the region around 40 ppm we observed a substantial contribution of a slow decaying part. For this region a biexponential fit routine was used.

It is possible to follow the temperature dependence of the slow relaxing parts by applying difference spectroscopy and subtracting spectra with different recovery times. The lower trace in Fig. 1(a) shows such a difference spectrum. Besides the region around the isotropic shift of C₆₀ one finds additional intensity centered around 36 ppm. From the biexponential fit, we can estimate this slow relaxing contribution to be about 5–10 % of the total spectral intensity. The temperature dependence coincides with the points assigned to line 5. We therefore assign the slow relaxation rate to line 5. In Table I, the faster rate is tentatively assigned to peak 6, which is responsible for most of the intensity in this region. The relaxation rates of the different lines correlate with the measured hyperfine coupling constants. For a quantitative evaluation, however, also the hyperfine anisotropy has to be taken into account.

In order to prove the existence of sp^3 -type geometries in RbC₆₀, one also has to consider the anisotropy of the chemical shift tensor. For the investigation of shift anisotropy the magic angle turning (MAT) technique¹⁷ was applied. This two-dimensional (2D) technique allows us to correlate isotropic shift and anisotropic powder patterns using very slow spinning speeds. The MAT experiments were performed at a ¹³C Larmor frequency of 45.6 MHz and at a rotor speed of 200 Hz. For sensitivity reasons we used the MAT-180 sequence¹⁸ consisting of one 90° and six 180° pulses.

The 2D spectrum in Fig. 2 displays the result for the region from 0 to 300 ppm: along the first frequency axis the carbon sites are separated according to their isotropic chemical shift value, whereas the second frequency axis shows the corresponding (quasistatic) powder pattern, which contains

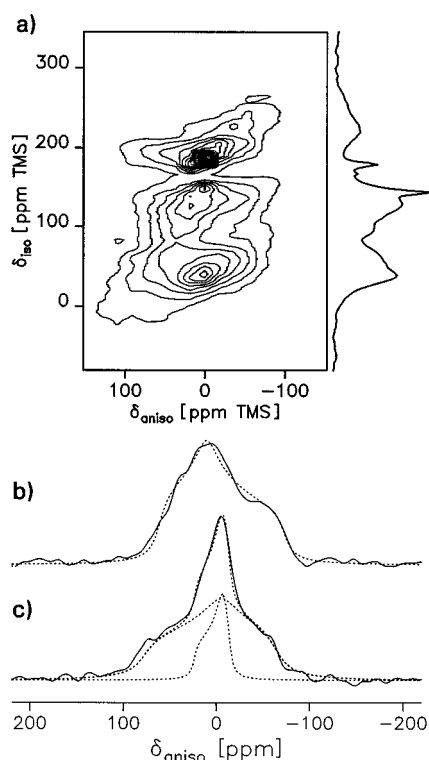


FIG. 2. (a) ^{13}C MAT-NMR experiment of RbC_{60} at $T=295\text{ K}$. For comparison a MAS spectrum is plotted along the isotropic axis of the spectrum. At the bottom the extracted anisotropy patterns of line 3 (b) and of the sp^3 region at 36 ppm (c) are shown. Dotted lines denote simulated powder patterns.

the anisotropy information. The anisotropy of lines with isotropic values below 150 ppm is clearly visible as can be seen in the 1D slices shown in Fig. 2. However, it turns out to be difficult to obtain quantitative results for lines 1 and 2. Their large anisotropy leads to a distribution of the spectral intensity over a large area of the 2D plot. Additional damping due to T_1 relaxation between the evolution times finally makes their anisotropy patterns disappear in the noise.

From the 2D spectrum it can also be concluded that on the experimental time scale of 10 ms the C_{60} molecules in the $\alpha\text{-C}_{60}$ and fcc phases are already rapidly reorienting. Their anisotropy patterns therefore are averaged to the isotropic

peaks at 143 and 179 ppm. The total width of the powder pattern of the low shift region is more than 100 ppm, which is much larger than expected for sp^3 carbons. The main contribution of the peak therefore has no sp^3 character and its shift is dominated by Knight shift, which is consistent with the variable temperature MAS and relaxation results.

In Fig. 2(b) we have plotted the anisotropy patterns of line 3 and those of the sp^3 region around 36 ppm. Despite several molecular sites contribute to the intensity of line 3, the anisotropy pattern can be approximated by an average tensor with the principal values of $[-68, 10, 58]$ (values in ppm). Concerning the sp^3 region, a fit with a single anisotropic powder pattern is not possible and one can clearly distinguish between at least two contributions with different anisotropies. The data is reproduced well by two tensors with the principal value $[-67, -7, 74]$ and $[-8, -15, 23]$. Whereas the first one has an anisotropy comparable to line 3, the latter has much smaller anisotropy similar to what would be expected for sp^3 carbons.

In summary, we used high-resolution NMR to map out the hyperfine coupling distribution on the C_{60} molecule in the polymer phase of RbC_{60} . The values obtained provide evidence for a large spin-density distribution on the C_{60} molecule in the polymeric phase. Since the hyperfine interaction reflects the electron spin density its distribution can be considered as a benchmark for electronic structure calculations. We also found a spectral contribution with all the features of sp^3 carbons: an isotropic chemical shift value near 40 ppm, small chemical shift anisotropy, small hyperfine coupling, and therefore only slow relaxation. This spectral feature even has the expected intensity. The main part of the spectrum, however, exhibits positive as well as negative Knight shifts and correspondingly short T_1 relaxation times. The weak temperature dependence of the T_1 relaxation can be interpreted in terms of antiferromagnetic coupling between the conduction electrons.¹⁹

The experimental findings confirm theoretical calculations,²⁰ where the C_{60} molecules are connected by insulating contacts and the electron transport is dominated by interchain hopping. Despite the one-dimensional chain structure of the C_{60} molecules, the electronic structure of RbC_{60} has therefore probably three-dimensional character.

Financial support by the Deutsche Forschungsgemeinschaft and the Fonds der Chemischen Industrie is gratefully acknowledged.

¹J. Winter and H. Kuzmany, *Solid State Commun.* **84**, 935 (1992).

²D. M. Poirier and J. H. Weaver, *Phys. Rev. B* **47**, 10 959 (1993).

³A. Jánossy, O. Chauvet, S. Pekker, J. R. Cooper, and L. Forró, *Phys. Rev. Lett.* **71**, 1091 (1993).

⁴Q. Zhu, O. Zhou, J. E. Fischer, A. R. McGhie, W. J. Romanow, R. M. Strongin, M. A. Cichy, and A. B. Smith, *Phys. Rev. B* **47**, 13 948 (1993).

⁵P. W. Stephens, G. Bortel, M. Tegze, A. Jánossy, S. Pekker, G. Oszlányi, and L. Forró, *Nature* **370**, 636 (1994).

⁶M. C. Martin, D. Koller, D. Xiaouqun, W. Stephens, and L. Mihály, *Phys. Rev. B* **49**, 10 818 (1994).

⁷O. Chauvet, G. Oszlányi, L. Forró, P. W. Stephens, M. Tegze, G. Faigel, and A. Jánossy, *Phys. Rev. Lett.* **72**, 2721 (1994).

⁸Q. Zhu, D. E. Cox, and J. E. Fischer, *Phys. Rev. B* **51**, 3966 (1995).

⁹P. Petit, J. Robert, and J. E. Fischer, *Phys. Rev. B* **51**, 11 924 (1995).

¹⁰G. Oszlányi, G. Bortel, G. Faigel, M. Tegze, L. Gránásy, S. Pekker, P. W. Stephens, G. Bendele, R. Dinnebier, G. Mihály, A. Jánossy, O. Chauvet, and L. Forró, *Phys. Rev. B* **51**, 12 228 (1995).

¹¹T. Kälber, G. Zimmer, and M. Mehring, *Z. Phys. B* **27**, 2 (1995).

¹²H. Alloul, V. Brouet, Y. Yoshinari, L. Malier, E. Lafontaine, and L. Forró, in *Physics and Chemistry of Fullerenes and Derivatives*, Proceedings of the IWEP NM95, edited by H. Kuzmany, J.

- Fink, M. Mehring, and S. Roth (World Scientific, Singapore, 1995), p. 443.
- ¹³G. Zimmer, M. Helmle, M. Mehring, F. Rachdi, J. Reichenbach, L. Firleij, and P. Bernier, *Europhys. Lett.* **24**, 59 (1993).
- ¹⁴T. Michael Duncan, *A Compilation of Chemical Shift Anisotropies* (Farragut, Chicago, 1990), p. C-4.
- ¹⁵T. Kälber, G. Zimmer, and M. Mehring, *Phys. Rev. B* **51**, 16 471 (1995).
- ¹⁶V. Brouet, H. Alloul, V. Brouet, Y. Yoshinari, and L. Forró, in *Physics and Chemistry of Fullerenes and Derivatives* (Ref. 12), p. 366.
- ¹⁷Z. Gan, *J. Am. Chem. Soc.* **114**, 8307 (1992).
- ¹⁸S. L. Gann, J. H. Baltisberger, and A. Pines, *Chem. Phys. Lett.* **210**, 405 (1993).
- ¹⁹M. Mehring, T. Kälber, U. Ludwig, K. F. Thier, and G. Zimmer, in *Physics and Chemistry of Fullerenes and Derivatives* (Ref. 12), p. 360.
- ²⁰S. C. Erwin, G. V. Krishna, and E. J. Mele, *Phys. Rev. B* **51**, 7345 (1995).